Available online at www.sciencedirect.com
SCIENCE DIRECT®
ELSEVIER
International Journal of Solids and Structures 42 (2005) 3677–3699
INTERNATIONAL JOURNAL OF SOLIDS and STRUCTURES
www.elsevier.com/locate/ijsolstr

Micro–macro analysis of shape memory alloy composites

S. Marfia *

Department of Mechanics, Structures and Environment, University of Cassino, Via G. di Biasio 43, Cassino 03043, Italy

Received 25 October 2004
Available online 21 January 2005

Abstract

The aim of the paper is to develop a micro–macro approach for the analysis of the mechanical behavior of composites obtained embedding long fibers of Shape Memory Alloys (SMA) into an elastic matrix. In order to determine the overall constitutive response of the SMA composites, two homogenization techniques are proposed: one is based on the self-consistent method while the other on the analysis of a periodic composite. The overall response of the SMA composites is strongly influenced by the pseudo-elastic and shape memory effects occurring in the SMA material. In particular, it is assumed that the phase transformations in the SMA are governed by the wire temperature and by the average stress tensor acting in the fiber. A possible prestrain of the fibers is taken into account in the model.

Numerical applications are developed in order to analyze the thermo-mechanical behavior of the SMA composite. The results obtained by the proposed procedures are compared with the ones determined through a micromechanical analysis of a periodic composite performed using suitable finite elements.

Then, in order to study the macromechanical response of structural elements made of SMA composites, a three-dimensional finite element is developed implementing at each Gauss point the overall constitutive laws of the SMA composite obtained by the proposed homogenization procedures. Some numerical applications are developed in order to assess the efficiency of the proposed micro–macro model.

Keywords: Micro–macro approach; Shape memory alloy; Composites; Homogenization; Self-consistent; Numerical procedures; Finite elements

1. Introduction

The shape memory alloy, often indicated by the acronym SMA, represents one of the most interesting smart material, more and more adopted in structural engineering applications. In fact, SMA possesses two

* Tel.: +397762993745; fax: +397762993392.
E-mail address: marfia@unicas.it

0020-7683/$ - see front matter © 2004 Elsevier Ltd. All rights reserved.
doi:10.1016/j.ijsolstr.2004.11.020

unique abilities: the capacity to recover large strains and to generate internal forces during their activation, during cycles of stress and temperature. These very special capabilities arise from the so-called pseudo-elastic and shape memory effects. Several three-dimensional models have been proposed in literature to study the mechanical response of shape memory alloys. Among others, Boyd and Lagoudas (1996) presented a model thermodynamically consistent, taking into account the SMA phase transformations and the reorientation process. Raniecki and Lexcellent (1998) developed a thermodynamically consistent model considering the pseudo-elastic behavior. Souza et al. (1998) proposed a thermodynamically consistent model able to catch most of the significant SMA macroscopic features, such as, the shape memory and pseudo-elastic effect, the asymmetric tension–compression response and the thermomechanical coupling. Auricchio and Petrini (2002, 2004) developed a robust integration algorithm for the model proposed by Souza et al. (1998) to be adopted into a finite element code for the analysis of SMA structural elements.

In order to guaranty adequate stiffness and ultimate strength of structural elements, together with high durability and long-term performances, SMAs are sometime embedded into a plastic or metallic matrix. In particular, advanced materials are obtained embedding the SMA in high performance composites, such as carbon or glass fiber reinforced materials. In fact, elements obtained from SMAs in the form of wires, strips, or tubes, integrated within, or bonded to, the composite material offer great capabilities for active control of the static and dynamic behavior of the overall integrated structures.

The overall behavior of SMA composite depends on the type and the quantity of adopted components; in fact, it is possible to design the material on the base of the particular mechanical, thermal, electric properties required for a specific application.

The possible use and the performances of the composite SMA integrated in structural elements can be studied using simplified constitutive laws for the composites according to which the detailed interaction of the SMA fibers with the surrounding matrix is neglected. In particular, several researchers have developed analytical (Lee and Choi, 1999), numerical (Lee et al., 1999; Ostachowicz et al., 2000) and experimental (Choi et al., 1999; Thompson and Loughlan, 2000) macromechanical studies of the thermal buckling behavior of laminated composite elements with embedded SMA wires, using the activation force of embedded SMA wire in order to increase the critical buckling temperature and reduced the thermal buckling deformation.

Some researches have been developed with the aim of designing the composite SMA considering the effective nonlinear mechanical properties of the constituents. In other words, a limited amount of papers have treated the micromechanics and the homogenization problem to derive the overall behavior of SMA composite.

Among others, Boyd et al. (1994) studied the interaction between the embedded SMA and the matrix in order to design the composites. Cherkaoui et al. (2000) developed a micromechanical analysis using the self-consistent homogenization technique to evaluate the overall SMA composite behavior. They investigated on the role of microstructure and constituent properties in the overall response of shape memory alloy composite. Kawai (2000) studied the effects of the inelastic deformation of the matrix on the overall behavior of a unidirectional TiNi SMA fiber composite and on the local pseudo-elastic response of the embedded SMA fibers under isothermal loading and unloading conditions. The average behavior of the SMA composite is evaluated with the micromechanical method of cells. Lu and Weng (2000) proposed a two-level micromechanical analysis in order to study the influence of the shape and the volume concentration of SMA inclusion on the overall behavior of SMA composite. The first level corresponds to the smaller SMA level where the phase transformations occur. The second level is the larger scale consisting of SMA inclusion in a polymeric matrix. Briggs and Ponte Castañeda (2002) studied the effective behavior of active composites, obtained embedding aligned SMA fibers in a linear elastic matrix, using the homogenization technique proposed by Ponte Castañeda (1991). Marfia and Sacco (2005) presented a micromechanical study of composite with embedded SMA fiber developing analytical and numerical homogenization procedures in order to determine the overall response of the composite.

The analysis of composite structures that involve embedded SMA materials should be based on overall constitutive relations that have to be established by a micromechanical approach. In other word, a micro–macro structural approach should be developed. The micro–macro approach is a complex task as in each point of the structures, suitable nonlinear homogenization techniques should be developed in order to evaluate the overall constitutive law of the composite on the basis of the mechanical properties of the components and of their interaction. For this reason, linked to the fact that the research on SMA composites has started only recently, a limited amount of studies have been addressed to the development of a micro–macro approach. Among others, Gilat and Aboudi (2004) proposed a micro–macro approach, adopting the SMA model of Lagoudas et al. (1996) to establish constitutive laws of unidirectional composite with a polymeric or metallic matrices and with embedded SMA fibers. To derive the overall constitutive behavior of the composite, the method of cells proposed by Paley and Aboudi (1992) was adopted. These micromechanically based constitutive equations are employed to study the response of plates made of composite SMA subjected to thermal loading.

The present work deals with the specific problem of developing a micro–macro approach for the determination of the mechanical response of structural elements made of SMA composite. First, suitable homogenization techniques are developed to determine the overall thermo-mechanical constitutive behavior of SMA composite considering the geometry of the composite and the specific properties of the components. In particular, an elastic matrix is considered and a computational efficient three-dimensional SMA model is adopted for the fibers. The adopted SMA model is based on the three-dimensional one proposed by Souza et al. (1998) and on the integration algorithm developed by Auricchio and Petrini (2002, 2004). It considers the phase transformations as function of stress and temperature, reproducing both the pseudo-elastic and the shape memory effects and the asymmetric tension-compression response.

The micromechanical behavior of SMA fibers in homogeneous elastic matrix is studied and analytical and numerical homogenization procedures are developed in order to evaluate the overall response of the composites characterized by random or periodic inclusions.

Concerning the analytical approach, a classical homogenization procedure, the self-consistent approach, appear to be suitable to derive the overall response, as the volume fraction of the SMA fiber in the composite generally assumes very low values, e.g. for 3–10%.

A numerical approach, based on the development of new finite elements, is proposed in order to study the response of periodic composites. In particular, the proposed finite elements are characterized by 3D displacement fields that do not vary along the fiber axis (Carvelli and Taliercio, 1999) and they are implemented in the numerical code FEAP (Zienkiewicz and Taylor, 1991).

Furthermore, a numerical micromechanical analysis of periodic composites is performed developing suitable finite elements for the SMA fiber and for the matrix.

Then, in order to study the macromechanical response of structural elements made of SMA composites, a micro–macro approach is proposed. In particular, a three-dimensional finite element is developed implementing the proposed homogenization techniques at the Gauss point level in order to evaluate the overall constitutive laws.

Numerical applications are developed to assess the capability of the proposed model and of the implemented numerical procedures. In particular, the results obtained by the analytical and numerical homogenization approaches are compared with the micromechanical results. Moreover, some numerical applications are performed to assess the efficiency of the proposed micro–macro approach.

In the following, first, the matrix and the fiber models are presented. Then, the analytical and numerical homogenization procedures and the micromechanical analysis are described. The proposed numerical procedure and solution algorithm are illustrated. Finally, some numerical results regarding the homogenization techniques, the micromechanical analysis and the micro–macro approach are presented.

2. Fiber and matrix material models

A representative volume element (RVE) of a composite material characterized by a volume V, with M and Ω the matrix and the inclusion volume, respectively, is considered.

The matrix material M is assumed homogeneous and characterized by a linear elastic constitutive law. In particular, the elastic strain in the matrix results:

$$\boldsymbol{\eta}^M = \boldsymbol{\varepsilon}^M - \boldsymbol{\tau} \tag{1}$$

with $\boldsymbol{\varepsilon}^M$ the total strain and $\boldsymbol{\tau}$ the inelastic strain. Thus, the stress–strain law is:

$$\boldsymbol{\sigma}^M = \mathbf{E}^M \boldsymbol{\eta}^M = \mathbf{E}^M(\boldsymbol{\varepsilon}^M - \boldsymbol{\tau}) \tag{2}$$

with $\boldsymbol{\sigma}^M$ the stress tensor and $\mathbf{E}^M$ the fourth-order elasticity tensor of the matrix. The inelastic strain $\boldsymbol{\tau}$ is due to a thermal deformation in the matrix and it is set as:

$$\boldsymbol{\tau} = \alpha^M(T - T_0)\mathbf{I} \tag{3}$$

where α^M is the expansion coefficient, T_0 is the reference temperature, T is the actual temperature and $\mathbf{I}$ is the second-order identity tensor.

For what concerns the inclusion constitutive model, the elastic strain is:

$$\boldsymbol{\eta}^\Omega = \boldsymbol{\varepsilon}^\Omega - \boldsymbol{\pi} \tag{4}$$

with $\boldsymbol{\varepsilon}^\Omega$ the total strain and $\boldsymbol{\pi}$ the inelastic strain, so that, the stress–strain law is:

$$\boldsymbol{\sigma}^\Omega = \mathbf{E}^\Omega \boldsymbol{\eta}^\Omega = \mathbf{E}^\Omega(\boldsymbol{\varepsilon}^\Omega - \boldsymbol{\pi}) \tag{5}$$

with $\boldsymbol{\sigma}^\Omega$ the stress tensor and $\mathbf{E}^\Omega$ the fourth-order elasticity tensor of the SMA inclusion. Introducing a coordinate system $(0, x_1, x_2, x_3)$ with the versor $\mathbf{k}^3$ in the direction of the fiber, the inelastic strain is written in the form:

$$\boldsymbol{\pi} = \alpha^\Omega(T - T_0)\mathbf{I} + \delta\mathbf{k}^3 \otimes \mathbf{k}^3 + \mathbf{d}^{\mathrm{t}} \tag{6}$$

i.e. the inelastic strain is obtained as the sum of three effects: the thermal expansion with α^Ω the expansion coefficient of the SMA, the possible prestrain δ of the SMA wire in the direction of the fiber and the transformation strain $\mathbf{d}^{\mathrm{t}}$.

For what concerns the SMA constitutive law, the model proposed by Souza et al. (1998) and modified by Auricchio and Petrini (2002, 2004) is adopted; it considers the pseudo-elastic effect, as well as the shape memory effect and the asymmetric tension-compression response. In the following the model is briefly described.

According to experimental evidence, it is assumed that the second-order strain tensor $\mathbf{d}^{\mathrm{t}}$ associated to the phase transformations is traceless so that no volume changes occur during the phase transition. It can be pointed out that the model, characterized by only one single internal variable $\mathbf{d}^{\mathrm{t}}$, is able to simulate a generic parent phase associated to no macroscopic strain and a generic product phase associated to macroscopic strain. The model is not able to distinguish between austenite and twinned martensite, since both phases do not produce any macroscopic strain. The internal variable $\mathbf{d}^{\mathrm{t}}$ is set as:

$$0 \leqslant \|\mathbf{d}^{\mathrm{t}}\| \leqslant \varepsilon_L \tag{7}$$

where ε_L is a material parameter indicating the maximum transformation strain reached at the end of the transformation during an uniaxial test.

It is convenient to split the stress and the strain and the stress in the SMA as:

$$\boldsymbol{\varepsilon}^\Omega = \mathbf{d} + \frac{\vartheta}{3}\mathbf{I} \tag{8}$$

$$\boldsymbol{\sigma}^{\Omega} = \mathbf{s} + p\mathbf{I} \tag{9}$$

where $\mathbf{d}$ and $\vartheta = \boldsymbol{\varepsilon} \bullet \mathbf{I}$ are the deviatoric and the volumetric strain, $\mathbf{s}$ and $p = \boldsymbol{\sigma} \bullet \mathbf{I}/3$ are the deviatoric and volumetric stress and the symbol '•' indicates the scalar product. The model is thermodynamically consistent (Auricchio and Petrini, 2004). The constitutive relations can be written as:

$$p = k\vartheta \tag{10}$$

$$\mathbf{s} = 2G(\mathbf{d} - \mathbf{d}^{\mathrm{t}}) \tag{11}$$

with k and G the bulk and the shear modulus of the material. The thermodynamic force $\mathbf{X}$ associated to the transformation strain $\mathbf{d}^{\mathrm{t}}$ is expressed as:

$$\mathbf{X} = \mathbf{s} - \boldsymbol{\alpha} \tag{12}$$

where $\boldsymbol{\alpha}$ plays the role of the back stress and it set as:

$$\boldsymbol{\alpha} = \mathbf{s} - [\beta\langle T - M_{\mathrm{f}}\rangle + h\|\mathbf{d}^{\mathrm{t}}\| + \gamma]\frac{\partial\|\mathbf{d}^{\mathrm{t}}\|}{\partial\mathbf{d}^{\mathrm{t}}} \tag{13}$$

In Eq. (13) the parameter M_{f} represents the finishing temperature of the austenite-martensite phase transformation, β is a material parameter linked to the dependence of the critical stress on the temperature, $\langle \bullet \rangle$ is the positive part of the argument; h is a material parameter indicating the slope of the linear stress-transformation relation in the uniaxial case and γ is defined as:

$$\begin{aligned} &\gamma = 0 \quad \text{if } 0 \leqslant \|\mathbf{d}^{\mathrm{t}}\| \leqslant \varepsilon_L \\ &\gamma \geqslant 0 \quad \text{if } \|\mathbf{d}^{\mathrm{t}}\| = \varepsilon_L \end{aligned} \tag{14}$$

In order to model the asymmetric behavior of SMA in tension and compression, the following yield function is introduced:

$$F(\mathbf{X}) = \sqrt{2J_2} + m\frac{J_3}{J_2} - R \tag{15}$$

where $J_2 = 1/2(\mathbf{X}^2 \bullet \mathbf{I})$ and $J_3 = 1/3(\mathbf{X}^3 \bullet \mathbf{I})$ are the second and third invariant of the deviatoric tensor $\mathbf{X}$, R is the radius of the elastic domain in the deviatoric space and m is a material parameter with $m < 0.46$ in order to guarantee the limit surface convexity. The parameter R and m can be evaluated as:

$$R = 2\sqrt{\frac{2}{3}}\frac{\sigma_{\mathrm{c}}\sigma_{\mathrm{t}}}{\sigma_{\mathrm{c}} + \sigma_{\mathrm{t}}} \quad m = \sqrt{\frac{27}{2}}\frac{\sigma_{\mathrm{c}} - \sigma_{\mathrm{t}}}{\sigma_{\mathrm{c}} + \sigma_{\mathrm{t}}} \tag{16}$$

with σ_{t} and σ_{c} the uniaxial critical stress in tension and compression. The model is completed introducing the associative evolution law of $\mathbf{d}^{\mathrm{t}}$:

$$\dot{\mathbf{d}}^{\mathrm{t}} = \dot{\zeta}\frac{\partial F(\mathbf{X})}{\partial\boldsymbol{\sigma}^{\Omega}} \tag{17}$$

with $\dot{\zeta}$ the plastic multiplier and the Kuhn–Tucker conditions:

$$\dot{\zeta} \geqslant 0 \quad F \leqslant 0 \quad \dot{\zeta}F = 0 \tag{18}$$

3. Micromechanics and homogenization

The representative volume element of the composite material is subjected to an average strain $\bar{\mathbf{e}}$ and to the two inelastic strain fields $\boldsymbol{\tau}$ and $\boldsymbol{\pi}$ in the matrix and in the inclusion, respectively, which can take into account the following effects:

- $\bar{\mathbf{e}}$ arises from the applied stress;
- $\boldsymbol{\tau}$, introduced in the previous section, can be due to a possible thermal deformation of the matrix;
- $\boldsymbol{\pi}$, introduced in the previous section, accounts for the inelastic strain in the inclusion due to the austenite–martensite phase transformation and also to a thermal deformation.

The average strain $\bar{\mathbf{e}}$ induces a strain field $\mathbf{e}$ obtained by the relation:

$$\mathbf{e}(\mathbf{x}) = \mathbf{R}(\mathbf{x})\bar{\mathbf{e}} \tag{19}$$

where $\mathbf{R}(\mathbf{x})$ is a fourth-order tensor which allows to compute the strain at a point $\mathbf{x}$ of the composite due to the presence of the average strain $\bar{\mathbf{e}}$.

For what concerns the presence of the inelastic strains, $\boldsymbol{\tau}$ is assumed constant in the matrix and zero in the inclusion, while $\boldsymbol{\pi}$ is assumed constant in the inclusion and zero in the matrix. In particular, the effect of the inelastic strain $\boldsymbol{\tau}$, assumed constant in the matrix, can be studied as the superposition of $\boldsymbol{\tau}$ in the whole composite and $-\boldsymbol{\tau}$ in the inclusion.

Because of the inelastic strains $\boldsymbol{\tau}$ and $\boldsymbol{\pi}$, two strain fields $\mathbf{t}$ and $\mathbf{p}$ arise in the composite, which can be computed as:

$$\mathbf{t}(\mathbf{x}) = [\mathbf{I} - \mathbf{P}(\mathbf{x})]\boldsymbol{\tau} \quad \mathbf{p}(\mathbf{x}) = \mathbf{P}(\mathbf{x})\boldsymbol{\pi} \tag{20}$$

where $\mathbf{P}(\mathbf{x})$ is the fourth-order tensor which allows to compute the strain at a point $\mathbf{x}$ due to the presence of a inelastic strain in the inclusion. The total strain field in the composite is obtained taking into account Eqs. (19) and (20) as:

$$\boldsymbol{\varepsilon}(\mathbf{x}) = \mathbf{e}(\mathbf{x}) + \mathbf{t}(\mathbf{x}) + \mathbf{p}(\mathbf{x}) = \mathbf{R}(\mathbf{x})\bar{\mathbf{e}} + [\mathbf{I} - \mathbf{P}(\mathbf{x})]\boldsymbol{\tau} + \mathbf{P}(\mathbf{x})\boldsymbol{\pi} \tag{21}$$

The elastic strains in the matrix $\boldsymbol{\eta}^{eM}$, $\boldsymbol{\eta}^{\tau M}$ and $\boldsymbol{\eta}^{\pi M}$ and in the inclusion $\boldsymbol{\eta}^{e\Omega}$, $\boldsymbol{\eta}^{\tau\Omega}$ and $\boldsymbol{\eta}^{\pi\Omega}$, due to the presence of the average strain $\bar{\mathbf{e}}$ and the two inelastic strain $\boldsymbol{\tau}$ and $\boldsymbol{\pi}$, are given by the relations:

$$\begin{aligned}
&\boldsymbol{\eta}^{eM} = \mathbf{R}^{M}\bar{\mathbf{e}} \qquad \boldsymbol{\eta}^{e\Omega} = \mathbf{R}^{\Omega}\bar{\mathbf{e}} \\
&\boldsymbol{\eta}^{\tau M} = -\mathbf{P}^{M}\boldsymbol{\tau} \quad \boldsymbol{\eta}^{\tau\Omega} = -(\mathbf{P}^{\Omega} - \mathbf{I})\boldsymbol{\tau} \\
&\boldsymbol{\eta}^{\pi M} = \mathbf{P}^{M}\boldsymbol{\pi} \qquad \boldsymbol{\eta}^{\pi\Omega} = (\mathbf{P}^{\Omega} - \mathbf{I})\boldsymbol{\pi}
\end{aligned} \tag{22}$$

The constitutive equations for the matrix and the inclusion are, respectively:

$$\begin{aligned}
&\boldsymbol{\sigma}^{eM} = \mathbf{E}^{M}\mathbf{R}^{M}\bar{\mathbf{e}} \qquad \boldsymbol{\sigma}^{e\Omega} = \mathbf{E}^{\Omega}\mathbf{R}^{\Omega}\bar{\mathbf{e}} \\
&\boldsymbol{\sigma}^{\tau M} = -\mathbf{E}^{M}\mathbf{P}^{M}\boldsymbol{\tau} \quad \boldsymbol{\sigma}^{\tau\Omega} = -\mathbf{E}^{\Omega}(\mathbf{P}^{\Omega} - \mathbf{I})\boldsymbol{\tau} \\
&\boldsymbol{\sigma}^{\pi M} = \mathbf{E}^{M}\mathbf{P}^{M}\boldsymbol{\pi} \qquad \boldsymbol{\sigma}^{\pi\Omega} = \mathbf{E}^{\Omega}(\mathbf{P}^{\Omega} - \mathbf{I})\boldsymbol{\pi}
\end{aligned} \tag{23}$$

The average stress and strain in the composite material are defined as:

$$\bar{\boldsymbol{\sigma}} = \frac{1}{V}\left(\int_{\Omega}\boldsymbol{\sigma}^{\Omega}\,\mathrm{d}V + \int_{M}\boldsymbol{\sigma}^{M}\,\mathrm{d}V\right) = f^{\Omega}\bar{\boldsymbol{\sigma}}^{\Omega} + f^{M}\bar{\boldsymbol{\sigma}}^{M} \tag{24}$$

$$\bar{\boldsymbol{\varepsilon}} = \frac{1}{V}\left(\int_{\Omega}\boldsymbol{\varepsilon}^{\Omega}\,\mathrm{d}V + \int_{M}\boldsymbol{\varepsilon}^{M}\,\mathrm{d}V\right) = f^{\Omega}\bar{\boldsymbol{\varepsilon}}^{\Omega} + f^{M}\bar{\boldsymbol{\varepsilon}}^{M} \tag{25}$$

with $f^{\Omega} = \Omega/V$ and $f^{M} = M/V$ the volume fractions, and $\bar{\boldsymbol{\varepsilon}}^{\Omega}$, $\bar{\boldsymbol{\sigma}}^{\Omega}$ and $\bar{\boldsymbol{\varepsilon}}^{M}$, $\bar{\boldsymbol{\sigma}}^{M}$ the average strain and stress in the inclusion and matrix, respectively.

It can be emphasized that the elastic strain fields $\boldsymbol{\eta}^{\tau}$ and $\boldsymbol{\eta}^{\pi}$, due to inelastic strains $\boldsymbol{\tau}$ and $\boldsymbol{\pi}$, are characterized by null average, so that it results $\bar{\boldsymbol{\eta}}^{\tau} = \mathbf{0}$ and $\bar{\boldsymbol{\eta}}^{\pi} = \mathbf{0}$.

The overall behavior of a composite is described by the constitutive equation:

$$\bar{\boldsymbol{\sigma}} = \overline{\mathbf{E}}\bar{\mathbf{e}} \tag{26}$$

where $\overline{\mathbf{E}}$ is the overall fourth-order elastic tensor of the composite. Indeed, the total average strain is:

$$\bar{\boldsymbol{\varepsilon}} = \bar{\mathbf{e}} + \bar{\mathbf{p}} + \bar{\mathbf{t}} \tag{27}$$

with $\bar{\mathbf{t}}$ and $\bar{\mathbf{p}}$ the average strain tensors due to the inelastic strains $\boldsymbol{\tau}$ and $\boldsymbol{\pi}$, respectively:

$$\bar{\mathbf{t}} = (\mathbf{I} - \overline{\mathbf{P}})\boldsymbol{\tau} \quad \bar{\mathbf{p}} = \overline{\mathbf{P}}\boldsymbol{\pi} \tag{28}$$

where $\overline{\mathbf{P}}$ is the average of the tensor $\mathbf{P}$ in the whole volume V.

Finally, in order to derive the overall response of the composite, the fourth-order tensors $\overline{\mathbf{E}}$ and $\overline{\mathbf{P}}$ have to be computed. Moreover, considering the case of composite material characterized by nonlinear constitutive equations, as it occurs for SMA fibers embedded in an elastic matrix, the evaluation of the elastic strain in the inclusion is necessary to solve the evolutionary problem.

In the following, two homogenization techniques are developed assuming that the nonlinear response of the inclusion, i.e. the phase transformations, are governed by the average stress tensor, i.e. on the average elastic strain, in Ω. Because of Eqs. (22), it results:

$$\bar{\boldsymbol{\eta}}^{\Omega} = \overline{\mathbf{R}}^{\Omega}\bar{\mathbf{e}} + (\mathbf{I} - \overline{\mathbf{P}}^{\Omega})\boldsymbol{\tau} - (\mathbf{I} - \overline{\mathbf{P}}^{\Omega})\boldsymbol{\pi} \tag{29}$$

where $\overline{\mathbf{R}}^{\Omega}$ and $\overline{\mathbf{P}}^{\Omega}$ are the average of the tensors $\mathbf{R}$ and $\mathbf{P}$ in the inclusion Ω.

The first technique is based on the classical self-consistent homogenization procedure adopted to evaluate $\overline{\mathbf{E}}$, $\overline{\mathbf{P}}$, $\overline{\mathbf{R}}^{\Omega}$ and $\overline{\mathbf{P}}^{\Omega}$; it can be emphasized that the self-consistent technique should give very satisfactory results for low values of the volume fraction of the inclusion, as in the case of composite SMA.

The second technique proposed by Marfia and Sacco (2005) evaluates the quantities $\overline{\mathbf{E}}$, $\overline{\mathbf{P}}$, $\overline{\mathbf{R}}^{\Omega}$ and $\overline{\mathbf{P}}^{\Omega}$ solving the problem of periodic composites using the finite element method.

Moreover, a numerical micromechanical analysis of a periodic SMA composite is performed, developed suitable finite elements for the fiber and the matrix. It can be pointed out that in the micromechanical analysis the inelastic strain is not constant in the inclusion Ω and the phase transformations are governed by the local stress tensor in the SMA wires and not by its average in Ω as in the homogenization techniques.

3.1. Self-consistent procedure

The self-consistent method is adopted to estimate the overall properties of the representative element volume of the composite. The self-consistent method is derived on the original Eshelby's solution of the ellipsoidal inhomogeneity (Mura, 1987; Nemat-Nasser and Hori, 1999); it is able to take into account approximately the interaction between the inhomogeneities by embedding them in a medium characterized by the effective mechanical properties of the RVE. Thus, it is assumed that the inclusion Ω is embedded in an elastic matrix, which has the yet unknown overall moduli of the composite.

The effect of the heterogeneity of the composite cell, i.e. the variation of elastic moduli from the matrix to the inclusion, can be simulated introducing an eigenstrain in a homogeneous material characterized by the RVE elastic properties. This inelastic strain should be able to reproduce the stress state in the inclusion Ω. The study is developed considering separately the effects of the average strain $\bar{\mathbf{e}}$ and of the two inelastic strain $\boldsymbol{\tau}$ and $\boldsymbol{\pi}$. In particular, only the explicit case of the presence of $\boldsymbol{\pi}$ is analyzed, as it allows the computation of the tensor $\mathbf{P}^{\boldsymbol{\Omega}}$, which is involved also in the problem with $\boldsymbol{\tau}$.

3.1.1. Average strain $\bar{\mathbf{e}}$

The total strain in the inclusion is equal to the elastic strain:

$$\mathbf{e}^{\Omega} = \boldsymbol{\eta}^{e\Omega} = \mathbf{R}^{\Omega}\bar{\mathbf{e}} \tag{30}$$

The consistency equation gives:

$$\mathbf{E}^{\Omega}\mathbf{e}^{\Omega} = \overline{\mathbf{E}}(\mathbf{e}^{\Omega} - \mathbf{e}^{*}) \tag{31}$$

which results:

$$\mathbf{e}^{\Omega} = \mathbf{A}^{\Omega}\mathbf{e}^{*} \quad \text{with } \mathbf{A}^{\Omega} = (\overline{\mathbf{E}} - \mathbf{E}^{\Omega})^{-1}\overline{\mathbf{E}} \tag{32}$$

with $\mathbf{e}^{*}$ the eigenstrain. The solution of the Eshelby problem proves that the eigenstrain in a single ellipsoidal volume Ω is constant and, taking into account Eq. (30), it is given by the relation:

$$\mathbf{e}^{\Omega} - \bar{\mathbf{e}} = \mathbf{S}^{\Omega}\mathbf{e}^{*} \tag{33}$$

where $\mathbf{S}^{\Omega}$ the fourth-order Eshelby tensor for transversely isotropic matrix and cylinder inclusion is evaluated in Section 3.1.3 (Mura, 1987). Substituting formula (33) into Eq. (31), the eigenstrain $\mathbf{e}^{*}$ results:

$$\mathbf{e}^{*} = (\mathbf{A}^{\Omega} - \mathbf{S}^{\Omega})^{-1}\bar{\mathbf{e}} \tag{34}$$

Relations (30), (32) and (34) give:

$$\mathbf{R}^{\Omega} = \overline{\mathbf{R}}^{\Omega} = \mathbf{A}^{\Omega}(\mathbf{A}^{\Omega} - \mathbf{S}^{\Omega})^{-1} \tag{35}$$

From the average stress equation (24), taking into account relation (25), it results:

$$\begin{aligned}\overline{\mathbf{E}}\bar{\mathbf{e}} &= \bar{\boldsymbol{\sigma}}^{e}\\ &= f^{\Omega}\bar{\boldsymbol{\sigma}}^{e\Omega} + f^{M}\bar{\boldsymbol{\sigma}}^{eM}\\ &= f^{\Omega}\mathbf{E}^{\Omega}\bar{\mathbf{e}}^{\Omega} + f^{M}\mathbf{E}^{M}\bar{\mathbf{e}}^{M}\\ &= f^{\Omega}\mathbf{E}^{\Omega}\bar{\mathbf{e}}^{\Omega} + \mathbf{E}^{M}(\bar{\mathbf{e}} - f^{\Omega}\bar{\mathbf{e}}^{\Omega})\\ &= \mathbf{E}^{M}\bar{\mathbf{e}} + f^{\Omega}(\mathbf{E}^{\Omega} - \mathbf{E}^{M})\bar{\mathbf{e}}^{\Omega}\end{aligned} \tag{36}$$

which, in combination with (30) and (35), considering that the strain in the inclusion is constant, i.e. $\mathbf{e}^{\Omega} = \bar{\mathbf{e}}^{\Omega}$, gives the overall elastic tensor as:

$$\overline{\mathbf{E}} = \mathbf{E}^{M} + f^{\Omega}(\mathbf{E}^{\Omega} - \mathbf{E}^{M})\mathbf{R}^{\Omega} \tag{37}$$

3.1.2. Inelastic strain $\boldsymbol{\pi}$

The total strain and the elastic strains in the inclusion are:

$$\mathbf{p}^{\Omega} = \mathbf{P}^{\Omega}\boldsymbol{\pi} \quad \boldsymbol{\eta}^{\pi\Omega} = (\mathbf{P}^{\Omega} - \mathbf{I})\boldsymbol{\pi} \tag{38}$$

The consistency and the Eshelby equations give:

$$\begin{cases}\mathbf{p}^{\Omega} = \mathbf{A}^{\Omega}\mathbf{p}^{*} + \boldsymbol{\pi}\\ \mathbf{p}^{\Omega} - \bar{\mathbf{p}} = \mathbf{S}^{\Omega}(\boldsymbol{\pi} + \mathbf{p}^{*})\end{cases} \Rightarrow \begin{cases}\mathbf{p}^{*} = (\mathbf{A}^{\Omega} - \mathbf{S}^{\Omega})^{-1}[\bar{\mathbf{p}} + (\mathbf{S}^{\Omega} - \mathbf{I})\boldsymbol{\pi}]\\ \mathbf{p}^{\Omega} = \mathbf{A}^{\Omega}(\mathbf{A}^{\Omega} - \mathbf{S}^{\Omega})^{-1}[\bar{\mathbf{p}} + (\mathbf{S}^{\Omega} - \mathbf{I})\boldsymbol{\pi}] + \boldsymbol{\pi}\end{cases} \tag{39}$$

with $\mathbf{p}^{*}$ the eigenstrain. From the first equation of (38) and the last equation of (39), it results:

$$\mathbf{P}^{\Omega}\boldsymbol{\pi} = \mathbf{A}^{\Omega}(\mathbf{A}^{\Omega} - \mathbf{S}^{\Omega})^{-1}[\bar{\mathbf{p}} + (\mathbf{S}^{\Omega} - \mathbf{I})\boldsymbol{\pi}] + \boldsymbol{\pi} \tag{40}$$

i.e.

$$\bar{\mathbf{p}} = [(\mathbf{A}^{\Omega} - \mathbf{S}^{\Omega})(\mathbf{A}^{\Omega})^{-1}(\mathbf{P}^{\Omega} - \mathbf{I}) - (\mathbf{S}^{\Omega} - \mathbf{I})]\boldsymbol{\pi} \tag{41}$$

Setting the average stress equation (24) equal to zero, taking into account relation (25) and the strain in the inclusion constant, i.e. $\mathbf{p}^{\Omega} = \bar{\mathbf{p}}^{\Omega}$, it results:

$$\begin{aligned}\mathbf{0} = \bar{\boldsymbol{\sigma}}^{\pi} &= f^{\Omega}\bar{\boldsymbol{\sigma}}^{\pi\Omega} + f^{M}\bar{\boldsymbol{\sigma}}^{\pi M} \\ &= f^{\Omega}\mathbf{E}^{\Omega}(\bar{\mathbf{p}}^{\Omega} - \boldsymbol{\pi}) + f^{M}\mathbf{E}^{M}\bar{\mathbf{p}}^{M} \\ &= f^{\Omega}\mathbf{E}^{\Omega}(\bar{\mathbf{p}}^{\Omega} - \boldsymbol{\pi}) + \mathbf{E}^{M}(\bar{\mathbf{p}} - f^{\Omega}\bar{\mathbf{p}}^{\Omega}) \\ &= \mathbf{E}^{M}\bar{\mathbf{p}} + [f^{\Omega}(\mathbf{E}^{\Omega} - \mathbf{E}^{M})\mathbf{P}^{\Omega} - f^{\Omega}\mathbf{E}^{\Omega}]\boldsymbol{\pi}\end{aligned} \tag{42}$$

which gives:

$$\bar{\mathbf{p}} = -f^{\Omega}(\mathbf{E}^{M})^{-1}[(\mathbf{E}^{\Omega} - \mathbf{E}^{M})\mathbf{P}^{\Omega} - \mathbf{E}^{\Omega}]\boldsymbol{\pi} = \overline{\mathbf{P}}\boldsymbol{\pi} \tag{43}$$

Combining Eqs. (41) and (43), it applies:

$$\mathbf{P}^{\Omega} = \overline{\mathbf{P}}^{\Omega} = [(\mathbf{I} - \mathbf{S}^{\Omega}(\mathbf{A}^{\Omega})^{-1}) + f^{\Omega}((\mathbf{E}^{M})^{-1}\mathbf{E}^{\Omega} - \mathbf{I})]^{-1}[f^{\Omega}(\mathbf{E}^{M})^{-1}\mathbf{E}^{\Omega} + \mathbf{S}^{\Omega}(\mathbf{I} - (\mathbf{A}^{\Omega})^{-1})] \tag{44}$$

3.1.3. Evaluation of Eshelby tensor $\boldsymbol{S}^{\Omega}$

The Eshelby tensor for a transversely isotropic matrix and a cylinder inclusion is evaluated following the procedure proposed in Mura (1987). The typical component of the Eshelby tensor $\mathbf{S}^{\Omega}_{ijmn}$ can be expressed as:

$$\mathbf{S}^{\Omega}_{ijmn} = \frac{1}{8\pi}\mathbf{E}^{M}_{pqmn}(\overline{\mathbf{G}}_{ipjq} + \overline{\mathbf{G}}_{jpiq}) \tag{45}$$

where $\overline{\mathbf{G}}_{ijkl}$ depends on Green's functions and if the index occurs twice in any one term, summation is taken from 1 to 3. The nonzero components $\overline{\mathbf{G}}_{ijkl}$ for the special case, under consideration, i.e. a transversely isotropic matrix and a cylinder inclusion (Mura, 1987), are explicitly evaluated as:

$$\begin{aligned}&\overline{\mathbf{G}}_{1111} = \overline{\mathbf{G}}_{2222} = \frac{\pi(5\mathbf{E}^{M}_{1111} - 3\mathbf{E}^{M}_{1122})}{2(\mathbf{E}^{M}_{1111} - \mathbf{E}^{M}_{1122})\mathbf{E}^{M}_{1111}} && \overline{\mathbf{G}}_{1122} = \overline{\mathbf{G}}_{2211} = \frac{\pi(7\mathbf{E}^{M}_{1111} - \mathbf{E}^{M}_{1122})}{2(\mathbf{E}^{M}_{1111} - \mathbf{E}^{M}_{1122})\mathbf{E}^{M}_{1111}} \\ &\overline{\mathbf{G}}_{3311} = \overline{\mathbf{G}}_{3322} = \frac{2\pi}{\mathbf{E}^{M}_{2323}} && \overline{\mathbf{G}}_{1212} = -\frac{\pi(\mathbf{E}^{M}_{1111} + \mathbf{E}^{M}_{1122})}{2(\mathbf{E}^{M}_{1111} - \mathbf{E}^{M}_{1122})\mathbf{E}^{M}_{1111}} \\ &\overline{\mathbf{G}}_{3131} = \overline{\mathbf{G}}_{2323} = 0 && \overline{\mathbf{G}}_{3333} = \overline{\mathbf{G}}_{1133} = \overline{\mathbf{G}}_{2233} = 0\end{aligned} \tag{46}$$

Substituting the nonzero components $\overline{\mathbf{G}}_{ijkl}$, evaluated in (46), in formula (45) it results:

$$\begin{aligned}&\mathbf{S}^{\Omega}_{1111} = \mathbf{S}^{\Omega}_{2222} = \frac{5\mathbf{E}^{M}_{1111} + \mathbf{E}^{M}_{1122}}{8\mathbf{E}^{M}_{1111}} && \mathbf{S}^{\Omega}_{1122} = \mathbf{S}^{\Omega}_{2211} = -\frac{\mathbf{E}^{M}_{1111} - 3\mathbf{E}^{M}_{1122}}{8\mathbf{E}^{M}_{1111}} \\ &\mathbf{S}^{\Omega}_{1133} = \mathbf{S}^{\Omega}_{2233} = \frac{\mathbf{E}^{M}_{1133}}{2\mathbf{E}^{M}_{1111}} && \mathbf{S}^{\Omega}_{1212} = \frac{3\mathbf{E}^{M}_{1111} - \mathbf{E}^{M}_{1122}}{8\mathbf{E}^{M}_{1111}} \\ &\mathbf{S}^{\Omega}_{3131} = \mathbf{S}^{\Omega}_{2323} = \tfrac{1}{4} && \mathbf{S}^{\Omega}_{3333} = \mathbf{S}^{\Omega}_{3311} = \mathbf{S}^{\Omega}_{3322} = 0\end{aligned} \tag{47}$$

3.2. Periodic composite

A periodic composite obtained assembling an infinite number of repetitive parallelepiped unit cells V is considered. The unit cell is characterized by a parallelepiped shape with dimensions equal to $2a_1$, $2a_2$ and $2a_3$ parallel to the three coordinate axes x_1, x_2, x_3. The axis x_3 is parallel to the direction of the SMA fiber axis. In particular, the repetitive unit cell is obtained considering any possible value of a_3. The 3D displacement field for periodic media is expressed by the following representative form:

$$\mathbf{u}(x_1,x_2,x_3) = \bar{\boldsymbol{\varepsilon}}\mathbf{x} + \tilde{\mathbf{u}}(x_1,x_2,x_3) \tag{48}$$

where $\mathbf{x}$ is the position vector of the typical point of V, $\bar{\boldsymbol{\varepsilon}}$ is the average strain of the cell and $\tilde{\mathbf{u}}(x_1,x_2,x_3)$ is the periodic part of the displacement (Luciano and Sacco, 1998; Carvelli and Taliercio, 1999). From formula (48), the strain tensor is given by:

$$\boldsymbol{\varepsilon}(x_1,x_2,x_3) = \bar{\boldsymbol{\varepsilon}} + \tilde{\boldsymbol{\varepsilon}}(x_1,x_2,x_3) \tag{49}$$

where the tensor $\tilde{\boldsymbol{\varepsilon}}(x_1,x_2,x_3)$ is the periodic part of the strain, with null average in V, associated to the displacement $\tilde{\mathbf{u}}$.

As the thickness of the unit cell in the fiber direction can assume any value, imposing the periodicity and continuity conditions along the x_3-direction:

$$\tilde{\mathbf{u}}(x_1,x_2,a_3) = \tilde{\mathbf{u}}(x_1,x_2,-a_3) \quad \begin{matrix} \forall x_1 \in [-a_1,a_1] \\ \forall x_2 \in [-a_2,a_2] \end{matrix} \quad \forall a_3 \tag{50}$$

the displacement field results function only of x_1 and x_2 i.e. $\tilde{u}_i(x_1,x_2,x_3) = \tilde{u}_i(x_1,x_2)$. Thus, the in-plane periodicity and continuity conditions are:

$$\begin{aligned} &\tilde{\mathbf{u}}(a_1,x_2) = \tilde{\mathbf{u}}(-a_1,x_2) \quad \forall x_2 \in [-a_2,a_2] \\ &\tilde{\mathbf{u}}(x_1,a_2) = \tilde{\mathbf{u}}(x_1,-a_2) \quad \forall x_1 \in [-a_1,a_1] \end{aligned} \tag{51}$$

Because of the displacement representation formula (48), taking into account the condition (50), the strain field does not depend on the x_3-coordinate and it is:

$$\boldsymbol{\varepsilon} = \bar{\boldsymbol{\varepsilon}} + \begin{bmatrix} \hat{u}_{1,1} & \frac{1}{2}(\hat{u}_{1,2}+\hat{u}_{2,1}) & \frac{1}{2}\hat{u}_{3,1} \\ \frac{1}{2}(\hat{u}_{1,2}+\hat{u}_{2,1}) & \hat{u}_{2,2} & \frac{1}{2}\hat{u}_{3,2} \\ \frac{1}{2}\hat{u}_{3,1} & \frac{1}{2}\hat{u}_{3,2} & 0 \end{bmatrix} \tag{52}$$

A homogenization procedure based on the analysis of a periodic composite is proposed and described in detail in Marfia and Sacco (2005). The quantities $\overline{\mathbf{E}}$, $\overline{\mathbf{P}}$, $\overline{\mathbf{R}}^{\Omega}$ and $\overline{\mathbf{P}}^{\Omega}$ that characterized the composite response are evaluated by linear finite element analyses. To this aim a four-node finite element based on the cinematic hypotheses (50) and (51) with an elastic isotropic material is developed. In particular, the overall constitutive tensor $\overline{\mathbf{E}}$ and the localization tensor $\overline{\mathbf{R}}^{\Omega}$ are determined solving six elastic problems, each problem characterized by only one nonzero element of $\bar{\mathbf{e}}$. In a similar way the localization tensors $\overline{\mathbf{P}}$ and $\overline{\mathbf{P}}^{\Omega}$ are evaluated solving the six elastic problems obtained prescribing only one nonzero element of $\boldsymbol{\pi}$.

Furthermore, the micromechanical behavior of the periodic composite material subject to the mean strain state $\bar{\mathbf{e}}$, under the inelastic strains $\boldsymbol{\pi}$ in the inclusion and $\boldsymbol{\tau}$ in the matrix, is studied developing nonlinear finite element analyses of the periodic cell. In particular, the matrix is modeled with the finite elements, described above, characterized by an elastic isotropic material; the fiber is simulated implementing the nonlinear SMA model, presented in Section 2, in the proposed four node element, based on the cinematic hypotheses (50) and (51). It can be emphasized that the nonlinear finite element micromechanical analysis of the periodic composite is performed considering the thermomechanical behavior of the SMA fiber and the phase transformations governed by the local stress tensor and by the temperature.

4. Numerical procedure and solution algorithm

Assigning an average strain and a temperature history, the thermo-mechanical behavior of the SMA composite is evaluated solving the evolutive equations governing the shape memory alloys phase transformations through a step by step time integration algorithm. In particular, once the solution at the time t_n is determined, the solution at the current time $t_{n+1} = t_n + \Delta t$ is evaluated adopting a backward-Euler implicit

integration procedure (Simo and Hughes, 1998). In the following, the quantities with the subscript 'n' are related to the previous time step t_n, while the ones with no subscript are referred to the current step t_{n+1}. Moreover, Δ indicates the variable increment at the time step Δt.

The time discrete model is solved adopting return-map algorithm in order to determine the inelastic strain tensor $\mathbf{d}^{\mathrm{t}}$ related to the phase transformation in the SMA wires. For the phase transition phenomena, the return-map algorithm properly modified with respect to the one usually adopted for plasticity models is adopted (Auricchio and Petrini, 2004).

Considering an average strain $\bar{\boldsymbol{\varepsilon}}$ and a temperature history T, the proposed numerical procedure is reported schematically for $\delta = 0$.

The overall properties of the SMA composite $\overline{\mathbf{E}}$, $\overline{\mathbf{P}}$, $\overline{\mathbf{R}}^{\Omega}$ and $\overline{\mathbf{P}}^{\Omega}$ are computed adopting the self-consistent procedure, described in Section 3.1, or the periodic composite procedure, illustrated in Section 3.2.

The finite time step is solved adopting the following algorithm. All the quantities involved in the solution algorithm, i.e. the stress $\bar{\boldsymbol{\sigma}}^{\Omega}$, the back-stress $\mathbf{X}$, the volumetric ϑ and deviatoric $\mathbf{d}$ part of the elastic strain, the inelastic strain $\mathbf{d}^{\mathrm{t}}$, etc., are considered constant in the inclusion.

The stress tensor in the SMA from Eqs. (5), (6), (27)–(29) is evaluated:

$$\begin{aligned}\bar{\boldsymbol{\sigma}}^{\Omega} &= \mathbf{E}^{\Omega}\bar{\boldsymbol{\eta}}^{\Omega} = \mathbf{E}^{\Omega}\left[\overline{\mathbf{R}}^{\Omega}\bar{\mathbf{e}} + (\mathbf{I}-\overline{\mathbf{P}}^{\Omega})\boldsymbol{\tau} - (\mathbf{I}-\overline{\mathbf{P}}^{\Omega})\boldsymbol{\pi}\right] = \mathbf{E}^{\Omega}\left[\overline{\mathbf{R}}^{\Omega}\bar{\boldsymbol{\varepsilon}} + (\overline{\mathbf{P}}-\overline{\mathbf{P}}^{\Omega})\boldsymbol{\tau} - (\mathbf{I}-\overline{\mathbf{P}}^{\Omega}+\overline{\mathbf{P}})\boldsymbol{\pi}\right]\\ &= \mathbf{E}^{\Omega}\left[\overline{\mathbf{R}}^{\Omega}\bar{\boldsymbol{\varepsilon}} + (\overline{\mathbf{P}}-\overline{\mathbf{P}}^{\Omega})\boldsymbol{\tau} - (\mathbf{I}-\overline{\mathbf{P}}^{\Omega}+\overline{\mathbf{P}})(\alpha^{\Omega}(T-T^0)\mathbf{I}+\mathbf{d}^{\mathrm{t}})\right].\end{aligned} \tag{53}$$

The transformation strain tensor $\mathbf{d}^{\mathrm{t}}$ is evaluated developing a return-map algorithm proposed in Auricchio and Petrini (2002, 2004) for the case of homogeneous SMA materials and herein extended in the case of SMA composites. The time discrete equations of the SMA constitutive model, presented in Section 2, are written:

$$\begin{aligned}&\bar{\boldsymbol{\sigma}}^{\Omega} = \mathbf{E}^{\Omega}[\overline{\mathbf{R}}^{\Omega}\bar{\boldsymbol{\varepsilon}} + (\overline{\mathbf{P}}-\overline{\mathbf{P}}^{\Omega})\boldsymbol{\tau} - (\mathbf{I}-\overline{\mathbf{P}}^{\Omega}+\overline{\mathbf{P}})(\alpha^{\Omega}(T-T^0)\mathbf{I}+\mathbf{d}^{\mathrm{t}})]\\ &p = \frac{1}{3}\bar{\boldsymbol{\sigma}}^{\Omega} \quad \mathbf{I} = K[\vartheta - 3\alpha^{\Omega}(T-T_0)]\\ &\mathbf{s} = \bar{\boldsymbol{\sigma}}^{\Omega} - p\mathbf{I} = 2G(\mathbf{d}-\mathbf{d}^{\mathrm{t}})\\ &\mathbf{X} = \mathbf{s} - [\beta\langle T - M_{\mathrm{f}}\rangle + h\|\mathbf{d}^{\mathrm{t}}\| + \gamma]\frac{\partial\|\mathbf{d}^{\mathrm{t}}\|}{\partial\mathbf{d}^{\mathrm{t}}}\\ &\gamma \geqslant 0\\ &\|\mathbf{d}^{\mathrm{t}}\| \leqslant \varepsilon_L\\ &\mathbf{d}^{\mathrm{t}} = \mathbf{d}^{\mathrm{t}}_n + \Delta\zeta\frac{\partial F(\mathbf{X})}{\partial\bar{\boldsymbol{\sigma}}^{\Omega}}\\ &F(\mathbf{X}) = \sqrt{2J_2} + m\frac{J_3}{J_2} - r \leqslant 0\\ &\Delta\zeta \geqslant 0 \quad F(\mathbf{X})\Delta\zeta = 0\end{aligned} \tag{54}$$

with $\Delta\zeta = (\zeta - \zeta_n)$ the consistency parameter time integrated in the interval Δt. It can be pointed out that the transformation stress $\mathbf{X}$ results undefined when the transformation strain is null and its derivative is undefined. To overcome this problem, as proposed in Auricchio and Petrini (2004), the norm $\|\mathbf{d}^{\mathrm{t}}\|$ is substituted with formula:

$$\overline{\|\mathbf{d}^{\mathrm{t}}\|} = \|\mathbf{d}^{\mathrm{t}}\| - \frac{\xi^{(\xi+1)/\xi}}{\xi-1}(\|\mathbf{d}^{\mathrm{t}}\| + \xi)^{(\xi-1)/\xi} \tag{55}$$

with ξ a parameter that controls the smoothness of the regularized norm.

The time discrete model is solved with an elastic predictor inelastic corrector procedure. The elastic trial state obtained keeping constant the internal variables is:

$$\begin{aligned}
&\mathbf{d}^{\mathrm{t,TR}} = \mathbf{d}^{\mathrm{t}}_n \\
&\bar{\boldsymbol{\sigma}}^{\Omega,\mathrm{TR}} = \mathbf{E}^{\Omega}[\overline{\mathbf{R}}^{\Omega}\bar{\boldsymbol{\varepsilon}} + (\overline{\mathbf{P}} - \overline{\mathbf{P}}^{\Omega})\boldsymbol{\tau} - (\mathbf{I} - \overline{\mathbf{P}}^{\Omega} + \overline{\mathbf{P}})(\alpha^{\Omega}(T - T^0)\mathbf{I} + \mathbf{d}^{\mathrm{t,TR}})] \\
&\mathbf{s}^{\mathrm{TR}} = \bar{\boldsymbol{\sigma}}^{\Omega,\mathrm{TR}} - \left(\frac{1}{3}\bar{\boldsymbol{\sigma}}^{\Omega,\mathrm{TR}} \quad \mathbf{I}\right)\mathbf{I} = 2G(\mathbf{d} - \mathbf{d}^{\mathrm{t,TR}}) \\
&\boldsymbol{\alpha}^{\mathrm{TR}} = \left[\langle\beta(T - M_{\mathrm{f}})\rangle + h\overline{\|\mathbf{d}^{\mathrm{t,TR}}\|}\right]\frac{\partial\overline{\|\mathbf{d}^{\mathrm{t,TR}}\|}}{\partial\mathbf{d}^{\mathrm{t}}} \\
&\mathbf{X}^{\mathrm{TR}} = \mathbf{s}^{\mathrm{TR}} - \boldsymbol{\alpha}^{\mathrm{TR}} \\
&F^{\mathrm{TR}}(\mathbf{X}^{\mathrm{TR}}) = \sqrt{2J_2(\mathbf{X}^{\mathrm{TR}})} + m\frac{J_3(\mathbf{X}^{\mathrm{TR}})}{J_2(\mathbf{X}^{\mathrm{TR}})} - R.
\end{aligned} \tag{56}$$

Then, the admissibility of the trial function is verified. If the trial state is admissible, $F^{\mathrm{TR}} < 0$, the step is elastic; if the trial state is nonadmissible $F^{\mathrm{TR}} \geqslant 0$, the step is inelastic and the transformation strain has to be evaluated integrating the evolutionary equations. The inelastic step is solved by the following procedure.

First, it is assumed $\gamma = 0$ and Eqs. (54) are written in the residual form:

$$\begin{aligned}
&\mathbf{R}^{X} = \mathbf{X} - \mathbf{s}^{\mathrm{TR}} + 2G\Delta\zeta\frac{\partial F}{\partial\boldsymbol{\sigma}^{\Omega}} - [\beta\langle T - M_{\mathrm{f}}\rangle + h\overline{\|\mathbf{d}^{\mathrm{t}}\|}]\frac{\partial\overline{\|\mathbf{d}^{\mathrm{t}}\|}}{\partial\mathbf{d}^{\mathrm{t}}} = 0 \\
&R^{\Delta\zeta} = \sqrt{2J_2} + m\frac{J_3}{J_2} - R = 0
\end{aligned} \tag{57}$$

The system of seven Eqs. (57) is solved using a Newton–Raphson method. If the solution obtained is not admissible, i.e. $\overline{\|\mathbf{d}^{\mathrm{t}}\|} > \varepsilon_L$, it is considered $\gamma > 0$ and Eqs. (54) are rewritten in the following residual form:

$$\begin{aligned}
&\mathbf{R}^{X} = \mathbf{X} - \mathbf{s}^{\mathrm{TR}} + 2G\Delta\zeta\frac{\partial F}{\partial\boldsymbol{\sigma}^{\Omega}} - [\beta\langle T - M_{\mathrm{f}}\rangle + h\overline{\|\mathbf{d}^{\mathrm{t}}\|} + \gamma]\frac{\partial\overline{\|\mathbf{d}^{\mathrm{t}}\|}}{\partial\mathbf{d}^{\mathrm{t}}} = 0 \\
&R^{\Delta\zeta} = \sqrt{2J_2} + m\frac{J_3}{J_2} - R = 0 \\
&R^{\gamma} = \overline{\|\mathbf{d}^{\mathrm{t}}\|} - \varepsilon_L = 0
\end{aligned} \tag{58}$$

The eight equation system is solved adopting a Newton–Raphson method. The iterative Newton–Raphson method is based on the linearization of Eqs. (57) and (58). In particular, for system (58) it results:

$$\begin{Bmatrix} \mathbf{R}^{X}_{k+1} \\ R^{\Delta\zeta}_{k+1} \\ R^{\gamma}_{k+1} \end{Bmatrix} = \begin{Bmatrix} \mathbf{R}^{X}_{k} \\ R^{\Delta\zeta}_{k} \\ R^{\gamma}_{k} \end{Bmatrix} + \begin{bmatrix} \mathbf{R}^{X}_{,X} & \mathbf{R}^{X}_{,\Delta\zeta} & \mathbf{R}^{X}_{,\gamma} \\ \mathbf{R}^{\Delta\zeta}_{,X} & R^{\Delta\zeta}_{,\Delta\zeta} & R^{\Delta\zeta}_{,\gamma} \\ \mathbf{R}^{\gamma}_{,X} & R^{\gamma}_{,\Delta\zeta} & R^{\gamma}_{,\gamma} \end{bmatrix} \begin{Bmatrix} \delta\mathbf{X} \\ \delta\zeta \\ \delta\gamma \end{Bmatrix} = \mathbf{0} \tag{59}$$

with the subscripts 'k+1' indicating the quantities at the current iteration while the subscript 'k' the ones at the previous iteration, δ indicating the variable increment between the two iterations and $(\bullet)^{\beta}_{,\alpha}$ the derivative of the residual equation $(\bullet)^{\beta}$ with $\beta = \mathbf{X}, \Delta\zeta, \gamma$ respect to $\alpha = \mathbf{X}, \Delta\zeta, \gamma$ evaluated at the iteration k.

The consistent tangent tensor is evaluated differentiating the constitutive equation of the SMA (Auricchio and Petrini, 2004):

$$\overline{\mathbf{E}}^{\Omega}_{t} = \frac{\mathrm{d}\bar{\boldsymbol{\sigma}}^{\Omega}}{\mathrm{d}\bar{\boldsymbol{\varepsilon}}^{\Omega}} = K(\mathbf{I}\otimes\mathbf{I}) + 2G(\mathbf{I} - \widehat{\mathbf{E}})\mathbf{I}_{\mathrm{dev}} \tag{60}$$

with

$$\widehat{\mathbf{E}} = \frac{\mathrm{d}\mathbf{d}^{\mathrm{t}}}{\mathrm{d}\mathbf{d}} = \begin{bmatrix} \mathbf{d}^{\mathrm{t}}_{,\mathbf{X}} & \mathbf{d}^{\mathrm{t}}_{,\Delta\zeta} & \mathbf{0} \end{bmatrix} \begin{bmatrix} \mathbf{R}^{X}_{,X} & \mathbf{R}^{X}_{,\Delta\zeta} & \mathbf{R}^{X}_{,\gamma} \\ \mathbf{R}^{\Delta\zeta}_{,X} & R^{\Delta\zeta}_{,\Delta\zeta} & R^{\Delta\zeta}_{,\gamma} \\ \mathbf{R}^{\gamma}_{,X} & R^{\gamma}_{,\Delta\zeta} & R^{\gamma}_{,\gamma} \end{bmatrix}^{-1} \begin{bmatrix} 2G\mathbf{I} \\ \mathbf{0} \\ \mathbf{0} \end{bmatrix}$$
$$\mathbf{I}_{\mathrm{dev}} = \mathbf{I} - \frac{1}{3}(\mathbf{I} \otimes \mathbf{I}) \tag{61}$$

Once the transformation strain $\mathbf{d}^{\mathrm{t}}$ in the SMA fibers is evaluated, the average stress in the SMA is computed from formula (53) and the average stress in the composite is evaluated from Eqs. (26)–(28) as

$$\bar{\boldsymbol{\sigma}} = \overline{\mathbf{E}}[\bar{\boldsymbol{\varepsilon}} - \overline{\mathbf{P}}(\alpha^{\Omega}(T - T_0)\mathbf{I} + \mathbf{d}^{\mathrm{t}}) - (\mathbf{I} - \overline{\mathbf{P}})\boldsymbol{\tau}]. \tag{62}$$

The tangent stiffness matrix of the SMA composite consistent with the developed algorithm is evaluated by differentiating of the constitutive equation (62) setting $T = T_0$:

$$\overline{\mathbf{E}}^{\mathrm{t}} = \frac{\mathrm{d}\bar{\boldsymbol{\sigma}}}{\mathrm{d}\bar{\boldsymbol{\varepsilon}}} = \overline{\mathbf{E}}\left[\mathbf{I} - \overline{\mathbf{P}}\frac{\mathrm{d}\mathbf{d}^{\mathrm{t}}}{\mathrm{d}\bar{\boldsymbol{\varepsilon}}}\right] \tag{63}$$

where

$$\frac{\mathrm{d}\mathbf{d}^{\mathrm{t}}}{\mathrm{d}\bar{\boldsymbol{\varepsilon}}} = \frac{\mathrm{d}\mathbf{d}^{\mathrm{t}}}{\mathrm{d}\mathbf{d}}\frac{\mathrm{d}\mathbf{d}}{\mathrm{d}\bar{\boldsymbol{\varepsilon}}^{\Omega}}\frac{\mathrm{d}\bar{\boldsymbol{\varepsilon}}^{\Omega}}{\mathrm{d}\bar{\boldsymbol{\varepsilon}}} = \widehat{\mathbf{E}}\mathbf{I}_{\mathrm{dev}}\overline{\mathbf{R}}^{\Omega}. \tag{64}$$

In order to develop a macromechanical analysis of SMA composite integrated in structural elements, a three-dimensional finite element is developed and implemented in the finite element code FEAP. In particular, the homogenization procedures, based on the self-consistent and on the periodic composite approaches, are implemented at the Gauss point level to model the SMA composite constitutive behavior.

5. Numerical results

To validate the proposed homogenization procedures some comparisons between the results obtained by the self-consistent approach, described in Section 3.1, by the homogenization technique based on the analyses of periodic media, proposed in Marfia and Sacco (2005), and briefly described in Section 3.2 and by the micromechanical analysis of periodic composites developed using the finite elements, proposed in Section 3.2, are carried out.

A composite characterized by a low stiffness polymeric matrix with Ni–Ti alloy fibers is considered. In particular, the material properties of the elastic matrix and of the SMA are:

- matrix:

$$E^{M} = 3600\ \mathrm{MPa} \quad \nu^{M} = 0.305 \quad \alpha^{M} = 0.0\ {}^{\circ}\mathrm{K}^{-1} \tag{65}$$

- SMA fiber:

$$\begin{array}{llll} E^{\Omega} = 53000\ \mathrm{MPa} & \nu^{\Omega} = 0.33 & \alpha^{\Omega} = 0.000001\ \mathrm{K}^{-1} & T_0 = 245\ \mathrm{K} \\ M_{\mathrm{f}} = 223\ \mathrm{K} & M_{\mathrm{s}} = 239\ \mathrm{K} & A_{\mathrm{s}} = 248\ \mathrm{K} & A_{\mathrm{f}} = 260\ \mathrm{K} \\ \beta = 2.1\ \mathrm{MPa\ K}^{-1} & \sigma_{\mathrm{c}} = 72\ \mathrm{MPa} & \sigma_{\mathrm{t}} = 56\ \mathrm{MPa} & \varepsilon_L^{(\pm)} = 0.04 \end{array} \tag{66}$$

where E^M, v^M, E^Ω and v^Ω are the Young modulus and the Poisson coefficient for the matrix and for the SMA, respectively, and the parameters M_s and M_f are the starting and finishing temperature of the austenite–martensite phase transformation in the case of stress-free material, A_s and A_f are the starting and finishing temperatures of the martensite–austenite phase transformation in the case of stress-free material and T_0 is the reference temperature.

In the following numerical applications, if not specified, a composite characterized by a fiber volume fraction equal to $f^\Omega = 0.1$ is considered. No prestrain in the fibers is considered.

5.1. Comparisons of the elastic moduli

In Tables 1 and 2 the homogenized elastic moduli evaluated by the self-consistent technique and by the homogenization procedure based on the analysis of periodic composites are reported for the fiber volume fraction equal to $f^\Omega = 0.05$ and to $f^\Omega = 0.1$, respectively. The values, reported in brackets for the self-consistent techniques, represent the differences respect to the results computed considering a periodic composite. It can be noted that the self-consistent technique is more accurate in the evaluation of the overall elastic moduli for the composite with the fiber volume fraction equal to $f^\Omega = 0.05$ than for the composite with $f^\Omega = 0.1$. In particular, for almost all the homogenized moduli, the differences reported in brackets for $f^\Omega = 0.05$ are one order of magnitude lower than the ones evaluated for $f^\Omega = 0.1$.

Furthermore, for both the analyzed values of the fiber volume fraction the difference in the evaluation of the shear homogenization moduli $\overline{\mathbf{E}}_{2323} = \overline{\mathbf{E}}_{1313}$ and $\overline{\mathbf{E}}_{1212}$ are significantly higher, one order of magnitude, than the differences in the computation of the other homogenized moduli.

It can be pointed that for what concerns the homogenized moduli $\overline{\mathbf{E}}_{1111} = \overline{\mathbf{E}}_{2222}$, $\overline{\mathbf{E}}_{1122}$, $\overline{\mathbf{E}}_{1133} = \overline{\mathbf{E}}_{2233}$ and $\overline{\mathbf{E}}_{3333}$ the results obtained by the two procedures can be considered in good accordance for both the analyzed values of the fiber volume fractions; while for shear moduli $\overline{\mathbf{E}}_{2323} = \overline{\mathbf{E}}_{1313}$ and $\overline{\mathbf{E}}_{1212}$ the self-consistent procedure results less accurate and for $f^\Omega = 0.1$ the differences respect to the results obtained considering a periodic composite appear significantly.

5.2. Pseudo-elastic effects

The mechanical response of the composite is analyzed when the pseudo-elastic effects occur in the SMA fibers. A loading–unloading history under constant temperature $T_0 = 285$ K is prescribed. In Fig. 1 the

Table 1
Homogenized elastic moduli [MPa] for $f^\Omega = 0.05$

	$\overline{\mathbf{E}}_{1111} = \overline{\mathbf{E}}_{2222}$	$\overline{\mathbf{E}}_{1122}$	$\overline{\mathbf{E}}_{1133} = \overline{\mathbf{E}}_{2233}$	$\overline{\mathbf{E}}_{3333}$	$\overline{\mathbf{E}}_{2323} = \overline{\mathbf{E}}_{1313}$	$\overline{\mathbf{E}}_{1212}$
Self-consistent technique	5700.52 (0.0004)	2786.98 (0.0014)	2817.63 (0.0008)	7940.10 (0.0004)	1591.25 (0.076)	1548.10 (0.062)
Periodic composite	5697.95	2782.96	2815.24	7936.22	1477.85	1457.55

Table 2
Homogenized elastic moduli [MPa] for $f^\Omega = 0.1$

	$\overline{\mathbf{E}}_{1111} = \overline{\mathbf{E}}_{2222}$	$\overline{\mathbf{E}}_{1122}$	$\overline{\mathbf{E}}_{1133} = \overline{\mathbf{E}}_{2233}$	$\overline{\mathbf{E}}_{3333}$	$\overline{\mathbf{E}}_{2323} = \overline{\mathbf{E}}_{1313}$	$\overline{\mathbf{E}}_{1212}$
Self-consistent technique	6120.83 (0.0039)	2968.83 (0.0042)	3035.50 (0.0043)	10567.90 (0.0008)	1900.69 (0.177)	1796.03 (0.144)
Periodic composite	6097.06	2956.31	3022.39	10559.43	1613.86	1570.44

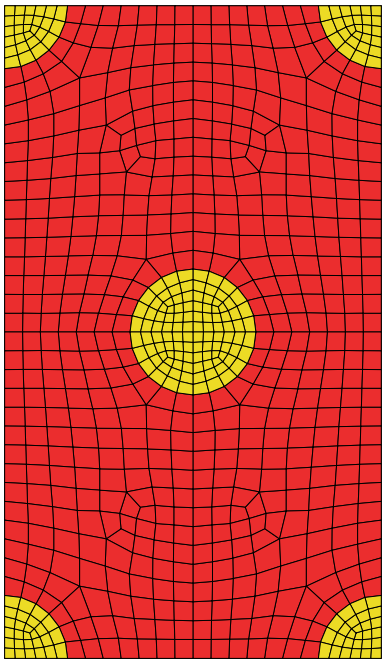

Fig. 1. Discretization of the periodic cell characterized by a fiber volume fraction equal to 0.1.

adopted discretization adopted for the periodic cell in the finite element analysis is represented. It can be pointed out that for the homogenization technique, based on the analysis of periodic composites, the quantities $\overline{\mathbf{E}}$, $\overline{\mathbf{P}}$, $\overline{\mathbf{R}}^{\Omega}$ and $\overline{\mathbf{P}}^{\Omega}$ are computed solving twelve linear elastic analyses of the periodic cell represented in Fig. 1, carried out considering both the matrix and the fibers linear elastic materials.

First the mechanical response in the direction of the fiber axis is investigated. The strain $\bar{\varepsilon}_{33}$ is increased until the value 0.04 is reached, then decreased to zero, keeping the other components of the overall deformation equal to zero.

In Fig. 2 the mechanical responses of the SMA composite in terms of the overall stress $\bar{\sigma}_{33}$ in the composite and of the stress in the SMA $\bar{\sigma}^{\Omega}_{33}$ versus $\bar{\varepsilon}_{33}$ is represented. The results obtained by the self-consistent and periodic cell homogenization techniques are denoted by 'Self-consistent' and 'Periodic Composite' respectively, and reported with dashed line and dashed–dotted line. It can be pointed out that the results in terms of overall mechanical response obtained using the two different homogenization procedures are in good accordance; thus, the differences reported in Table 2 are negligible for the examined value of the fiber volume fraction. Both the homogenization techniques are able to reproduce the response of SMA composite taking into account the phase transformations occurring in the SMA wires. It can be noted that both the austenite-martensite and martensite–austenite phase transformations occur in the SMA and at the end of the isothermal loading–unloading cycle the deformation is completely recovered. The response of the composite is significantly influenced by the pseudo-elastic effects in the SMA. In the same figure, a further comparison with the results obtained by the micromechanical analyses of the periodic cell represented in Fig. 1, developed using the finite elements, described in Section 3.2, is carried out; in particular an elastic isotropic material for the matrix and the SMA model presented in Section 2 for the fibers are adopted; this nonlinear finite element analyses is performed considering the phase transformations governed by the local normal stress tensor $\boldsymbol{\sigma}$ in the SMA wires. The results carried out by this procedure are reported in Fig. 2 with solid line and are denoted as 'FEM Periodic composite'. The micromechanical results evaluated

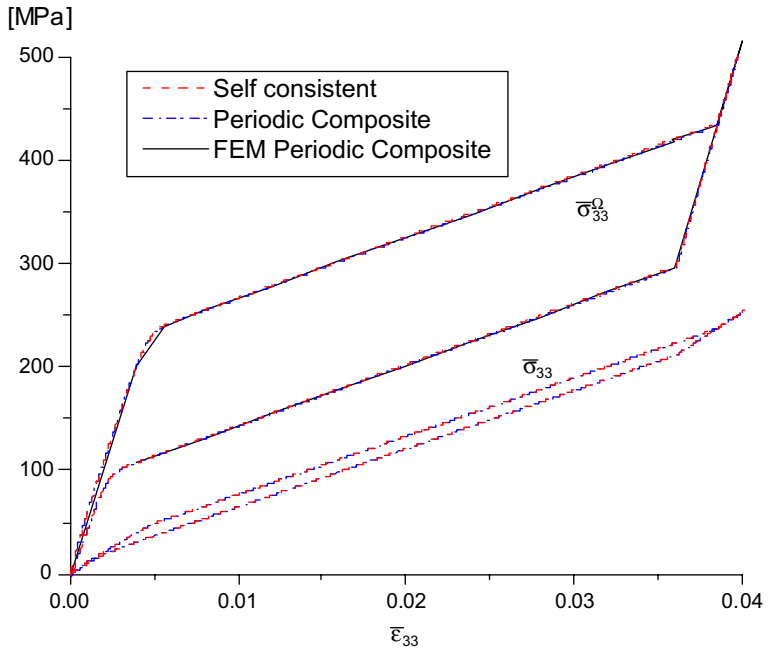

Fig. 2. Mechanical response of the SMA composites characterized by $f^{\Omega} = 0.1$ in the fiber axis direction: pseudo-elastic effects.

considering the phase transformations depending on the local stress tensor in the fiber, are in very good accordance with the ones obtained by the two proposed homogenization techniques where the phase transformations are governed by the average stress tensor in the wires. In Fig. 3, the distribution of the stress σ_{33} in the periodic cell is plotted when $\bar{\varepsilon}_{33} = 0.04$. It can be pointed out that the stress in the fiber is almost constant. Thus, it can be deduced that the simplifying assumption of governing the phase transformations by the average stress instead of the local stress is validated.

Then, the transversal mechanical response of the SMA composite, i.e. in a direction orthogonal respect to the fiber axis, is studied when pseudo-elastic effects occur in the SMA fibers. The strain $\bar{\varepsilon}_{23}$ is first increased until the value 0.08 is reached, then decreased to zero, keeping the other components of the overall deformation equal to zero.

In Fig. 4 the mechanical responses of the SMA composite in terms of the overall stress $\bar{\sigma}_{23}$ and of the stress in the SMA $\bar{\sigma}^{\Omega}_{23}$ versus $\bar{\varepsilon}_{23}$ is represented. The results obtained by the self-consistent, periodic cell homogenization techniques and by the nonlinear finite element micromechanical analysis are reported with dashed line, dashed–dotted line and solid line, respectively. It can be pointed out that the results obtained by the periodic cell homogenization and by the micromechanical analysis are in very good accordance both in terms of the overall stress and in terms of the stress in the SMA. The results obtained with the self-consistent procedure can be considered satisfactory in terms of the overall stress; on the other hand, significant differences appear in the evaluation of the stress in the SMA. These differences can be due to the fact that the self-consistent homogenization is less accurate in the evaluation of the shear overall moduli, as it has already underlined in Section 5.1 and in the determination of the transversal behavior of the composite. As final comment, it can be noted that also the transversal mechanical response of the composite is strongly influenced by the phase transformations occurring in the SMA fibers.

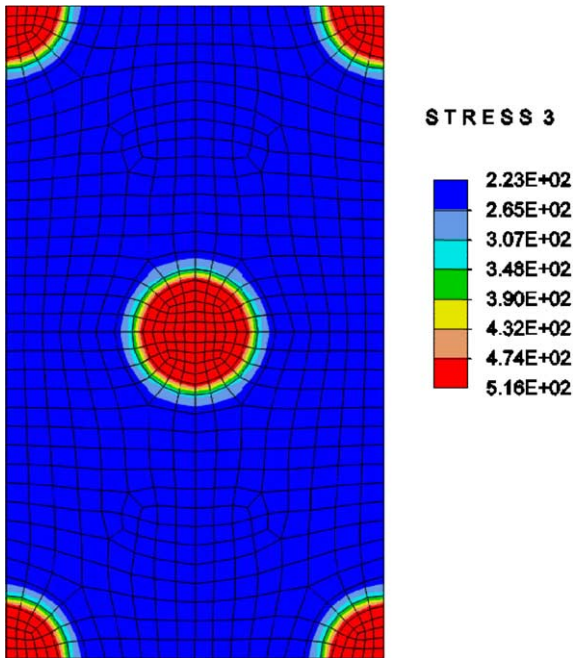

Fig. 3. Distribution of the stress σ_{33} in the periodic cell when $\bar{\varepsilon}_{33} = 0.04$.

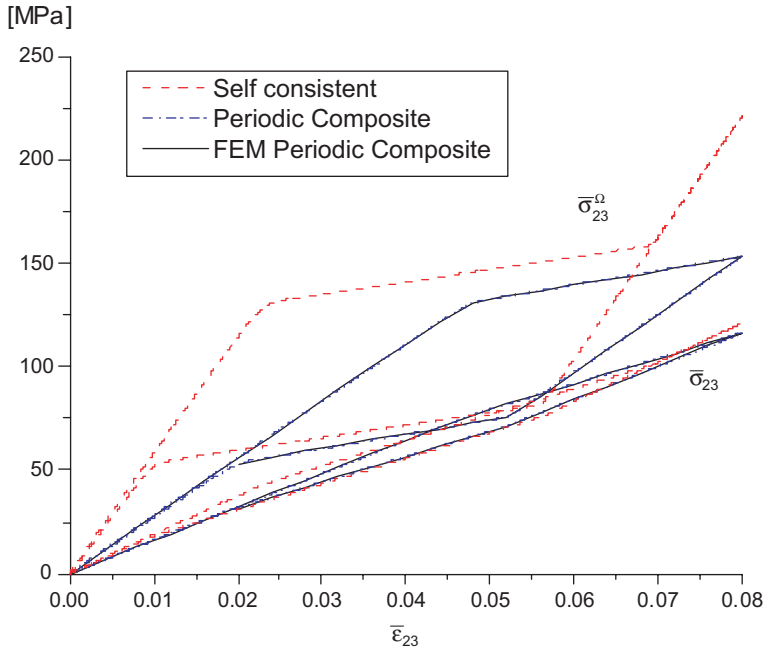

Fig. 4. Transversal mechanical response of the SMA composites characterized by $f^{\Omega} = 0.1$: pseudo-elastic effects.

5.3. Shape memory effects

The mechanical behavior of the composite is studied when shape memory effects occur in the SMA wires. In particular, the transversal mechanical response of the composite is studied. The following loading–unloading history is considered, setting the reference temperature $T_0 = 223$ K:

t [s]	0	1	2	3	4
$\bar{\varepsilon}_{23}$	0	0.04	0.0045	0.00	0.00
T [K]	223	223	223	252	223

In Fig. 5 the transversal mechanical responses of the SMA composite in terms of the overall stress $\bar{\sigma}_{23}$ and the stress in the SMA $\bar{\sigma}^{\Omega}_{23}$ versus $\bar{\varepsilon}_{23}$ is represented. The results obtained by the periodic cell homogenization techniques and by the nonlinear finite element micromechanical analysis are reported with dashed–dotted line and solid line, respectively.

It can be pointed that the results determined by the periodic cell homogenization and by the micromechanical analysis are in very good accordance. When $t = 1$ s only the austenite-martensite phase transformation is partially developed in the SMA wires; from $t = 1$ s to $t = 2$ s an unloading phase is prescribed at constant temperature until the overall stress $\bar{\sigma}_{23}$ becomes equal to zero. From $t = 2$ s to $t = 3$ s the strain is decreased and the temperature is increased keeping the stress $\bar{\sigma}_{23}$ equal to zero, the martensite–austenite phase transformation occurs in the SMA fibers. At the end of the analyses $t = 4$ s, the initial conditions are completely recovered decreasing the temperature to the initial value. The mechanical response of the composite is strongly influenced by the thermomechanical behavior of the SMA fibers and in particular by the shape memory effects.

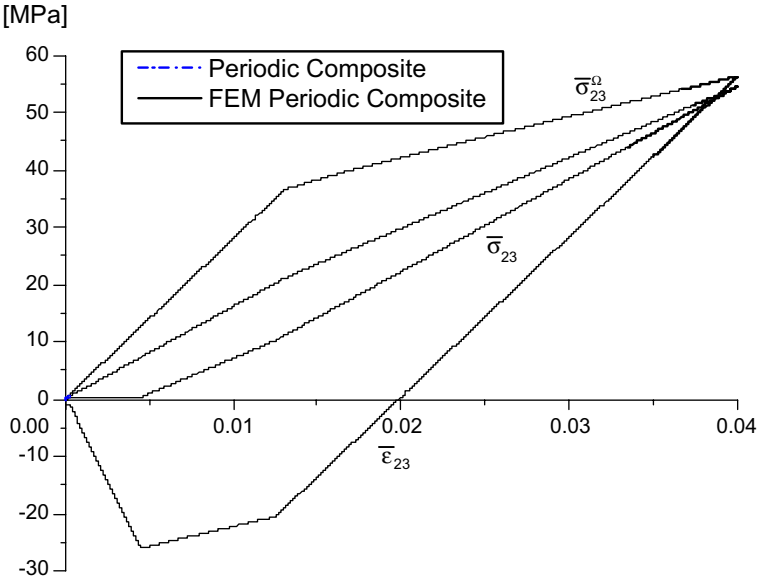

Fig. 5. Transversal mechanical response of the SMA composites characterized by $f^{\Omega} = 0.1$: shape memory effects.

5.4. Structural analysis

As the proposed homogenization procedures, based on the self-consistent method and on the periodic composites analysis, are able to determine the overall constitutive behavior for the SMA composites, they are implemented at the Gauss point level in a three-dimensional 8 node finite element in order to perform structural analyses and to design actuators made of SMA composites able to control the displacements and vibrations of structures.

An interesting application of a SMA laminate beam is presented. In particular the cantilever beam, represented in Fig. 6, is studied. The beam is characterized by a rectangular cross section with an elastic core and by two reinforcement layers made of SMA composite, one on the extrados and the other on the intrados of the beam. The SMA composite material properties are reported in (65) and (66). The geometrical properties of the beam are

$$L = 12 \text{ mm} \quad h = 1 \text{ mm} \quad h_R = 0.1 \text{ mm} \tag{67}$$

and material properties of the elastic core are

$$E_c = 4000 \text{ MPa} \quad v_c = 0.305 \tag{68}$$

A three-dimensional analyses of the beam is performed. The aim is to govern the transversal displacement of the cantilever beam performing temperature cycles in the SMA composite layers. To obtain phase transformation in the SMA wires by temperature changes, the beam is subjected first to a bending moment. The following loading history is applied

t [s]	0	1	2	3
M [N mm]	0	7.2	7.2	7.2
T [K]	223	223	600	223

Two different analyses are performed: one adopting the self-consistent homogenization technique and the other the periodic composite procedure in order to evaluate the overall constitutive law of the composite. The bending moment is applied at constant temperature and it is kept constant during the temperature changes in the SMA composite layers. In Fig. 7 the beam undeformed and deformed configurations are plotted; in particular the beam deformation at time $t = 1$ s, when the maximum value of the bending moment is reached at temperature $T = 223$ K and the austenite–martensite phase transformation has occurred in the SMA fibers, is reported. Then, an increasing temperature is applied at the two SMA composite layers and the reverse martensite–austenite phase transformation occurs in the SMA fibers, thus, as a consequence, the transversal displacement of the beam is reduced, as it can be noted in Fig. 7 where the beam deformed configuration at time $t = 2$ s, when $T = 600$ K, is plotted. From time $t = 2$ s to $t = 3$ s the temperature is decreased at the initial value and the beam goes back to the deformed shape of time $t = 1$ s,

Fig. 6. Cantilever beam reinforced with two layers of SMA composite: geometry, boundary and loading condition.

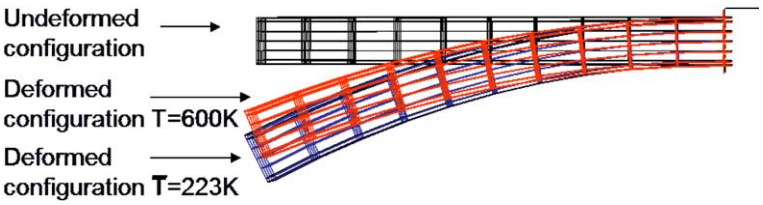

Fig. 7. Undeformed and deformed configurations of the cantilever beam subjected to bending and to thermal cyclic loading.

represented in Fig. 7. In Fig. 8 the transversal displacement of the free end cross section of the beam is plotted versus time. It can be noted that initially, the transversal displacement increases until the maximum value of the bending moment is reached, then the beam swings between two configurations: the beam is able to recover part of the transversal displacement during heating and it returns to the deformed shape during cooling.

In Fig. 9 the bending moment versus the transversal displacement is plotted. It can be pointed out that the first branch is nonlinear because of the nonlinear behavior of the SMA wires due to the phase transformations. Then, the bending moment is kept constant and changing the temperature the transversal displacement of the beam starts to oscillate between two values 0.606 mm and 0.477 mm.

In Figs. 8 and 9, the results obtained by the self-consistent homogenization technique and by the periodic cell homogenization procedure are reported with dashed line and solid line, respectively. It can be pointed that the results determined by the two homogenization techniques are in very good accordance. In fact, the SMA fibers in the composite layers are mainly subjected to a deformation in the direction of fiber axis, in this case, as it has already been pointed out in Sections 5.1 and 5.2, the results obtained by the two homogenization procedures are in good accordance.

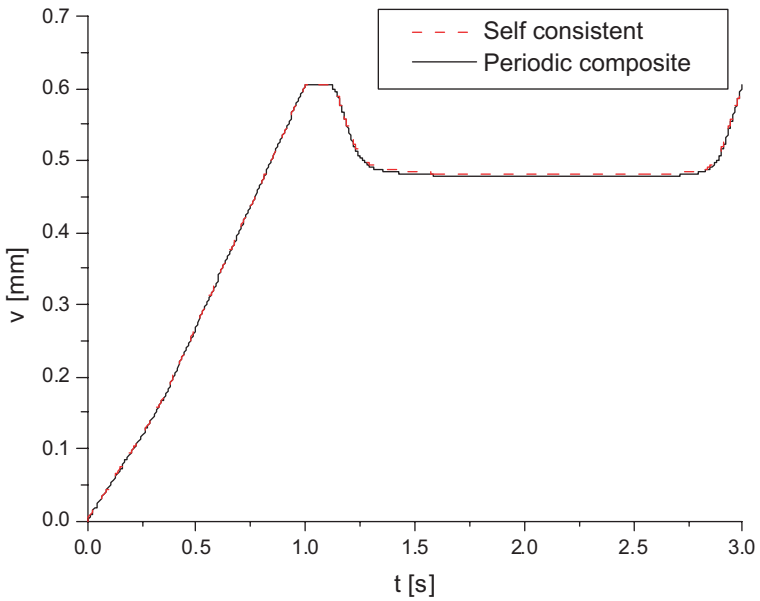

Fig. 8. Transversal displacement of the free end cross section of the cantilever beam versus time.

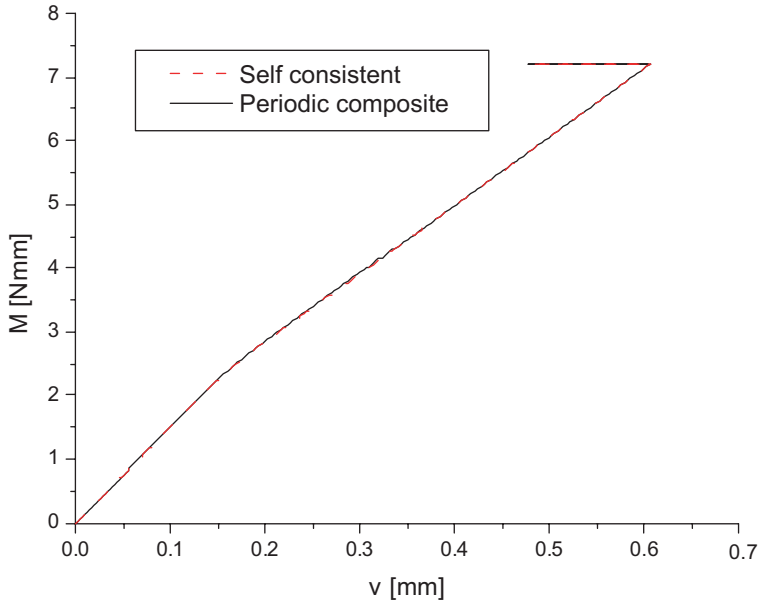

Fig. 9. Bending moment versus transversal displacement of the free end section of the cantilever beam.

6. Conclusions

A micro–macro approach for the analysis of composite obtained embedding SMA long fibers in an elastic matrix is presented. A three-dimensional model for the SMA material, that takes into account the thermomechanical behavior and the asymmetric tension–compression response, is adopted.

The overall constitutive behavior of the composite is evaluated developing two homogenization techniques: one based on the self-consistent method and the other on the analysis of periodic composite. It is assumed that the phase transformations are governed by the average stress tensor in the SMA wires. This assumption is validated comparing the results obtained by the homogenization procedures with the ones evaluated by a nonlinear finite element micromechanical analysis of a periodic composite.

The thermo-mechanical behavior of the SMA composite is evaluated solving the evolutive equations governing the shape memory alloys phase transformations developing a numerical procedure, based on the backward Euler integration scheme with a return-mapping algorithm. The proposed numerical procedure is stable, robust and it shows good convergence properties.

In order to perform a macromechanical structural analysis and to design actuators made of SMA composite, a three-dimensional finite element is developed implementing the two proposed homogenization procedures at the Gauss point level to evaluate the overall SMA composite constitutive behavior.

From the numerical results both the two homogenization procedures appear accurate in the evaluation of the overall composite response in the direction of the fiber axis. Some differences comes out in the determination of the composite overall behavior in a direction orthogonal to the fiber axis and they are due to the fact that the self-consistent technique is less accurate in the evaluation of the overall shear moduli and of the transversal response of the composite. It can be pointed out that the overall constitutive behavior of the SMA composite is strongly influenced by the pseudo-elastic and by the shape memory effects occurring in the SMA inclusions.

From the macromechanical analysis performed using the micro–macro approach it can be pointed out that the thermomechanical behavior of the SMA fibers significantly influences the response of the whole analyzed structure.

In particular, the micro–macro approach allows to determine the macromechanical response taking into account a constitutive relation directly derived from the micromechanical analysis, thus, taking into account the material properties of the composite constituents and their interaction. The micro–macro analysis is a fundamental point in the design of SMA composite as it can be used to analyze the influence of the volume fraction or of the material properties of the components on the macromechanical response of the structures reinforced with SMA layers for each particular application.

Acknowledgments

The present work has been partially developed within the joint French-Italian "Lagrangian Laboratory" with the financial support of the Italian Ministry of Education, University and Research (MIUR) in the framework of the PRIN project. The author wish to thank Prof. Sacco for the useful discussion on the nonlinear homogenization techniques.

References

Auricchio, F., Petrini, L., 2002. Improvements and algorithmical considerations on a recent three-dimensional model describing stress-induced solid phase transformation. International Journal for Numerical Methods in Engineering 55, 1255–1284.

Auricchio, F., Petrini, L., 2004. A three dimensional model describing stress–temperature induced solid phase transformations: solution algorithm and boundary value problems. International Journal for Numerical Methods in Engineering 61, 807–836.

Boyd, J., Lagoudas, D., 1996. A thermodynamical constitutive model for shape-memory materials. Part I. The monolithic shape-memory alloy. International Journal of Plasticity 12, 805–842.

Boyd, J., Lagoudas, D., Bo, Z., 1994. Micromechanics of active composites with SMA fibers. Journal of Engineering Materials and Tecnology 116, 1337–1347.

Briggs, P.J., Ponte Castañeda, P., 2002. Variational estimates for the effective response of shape memory alloy actuated fiber composites. Journal of Applied Mechanics 69, 470–480.

Carvelli, V., Taliercio, A., 1999. Micromechanical model for the analysis of unidirectional elasto-plastic composites subjected to 3D stresses. Mechanical Research Communications 26, 547–553.

Cherkaoui, M., Sun, Q.P., Song, G.Q., 2000. Micromechanics modeling of composite with ductile matrix and shape memory alloy reinforcement. International Journal of Solids and Structures 37, 1577–1594.

Choi, S., Lee, J.J., Seo, D.C., Choi, S.W., 1999. The active buckling control of laminated composite beams with embedded shape memory alloy wires. Composite Structures 47, 679–686.

Gilat, R., Aboudi, J., 2004. Dynamic response of active composites plates: shape memory alloy fibers in polymeric/metallic matrices. International Journal of Solids and Structures 41, 5717–5731.

Kawai, M., 2000. Effects of matrix inelasticity on the overall hysteretic behavior of TiNi-SMA fiber composites. International Journal of Plasticity 16, 263–282.

Lagoudas, D.C., Bo, Z., Qidwai, M.A., 1996. A unified thermodynamic constitutive model for SMA and finite element analysis of active metal matrix composites. Mechanics of Composite Materials and Structures 3, 153–179.

Lee, H.J., Lee, J.J., Huh, J.S., 1999. A simulation study on the thermal buckling behavior of laminated composite shells with embedded shape memory alloy (SMA) wires. Composite Structures 47, 463–469.

Lee, J.J., Choi, S., 1999. Thermal buckling and postbuckling analysis of a laminated composite beam with embedded SMA actuators. Composite Structures 47, 695–703.

Lu, Z.K., Weng, G.J., 2000. A two-level micromechanical theory for shape-memory alloy reinforced composite. International Journal of Plasticity 16, 1289–1307.

Luciano, R., Sacco, E., 1998. Variational methods for the homogenization of periodic media. European Journal of Mechanics A/Solids 17, 599–617.

Marfia, S., Sacco, E., 2005. Micromechanics and homogenization of SMA-wire reinforced materials. Journal of Applied Mechanics, 72.

Mura, T., 1987. Micromechanics of Defects in Solids, second revised ed. Martinus.
Nemat-Nasser, S., Hori, M., 1999. Micromechanics: Overall Properties of Heterogeneous Materials. North-Holland Elsevier.
Ostachowicz, W., Krawczuk, M., Zak, A., 2000. Dynamics and buckling of a multilayer composite plate with embedded SMA wires. Composite Structures 48, 163–167.
Paley, M., Aboudi, J., 1992. Micromechanical analysis of composites by the generalized cells method. Mechanics of Materials 14, 127–139.
Ponte Castañeda, P., 1991. The effective mechanical properties of nonlinear isotropic composites. Journal of the Mechanics and Physics of Solids 39, 45–71.
Raniecki, B., Lexcellent, Ch., 1998. Thermodynamics of isotropic pseudoelasticity in shape-memory alloys. European Journal of Mechanics A/Solids 17, 185–205.
Simo, J.C., Hughes, T.J.R., 1998. Computational Inelasticity. Springer-Verlag, New York.
Souza, A.C., Mamiya, E.N., Zouain, N., 1998. Three-dimensional model for solids undergoing stress-induced phase transformations. European Journal of Mechanics A/Solids 17, 789–806.
Thompson, S.P., Loughlan, J., 2000. The control of the post-buckling response in thin plates using smart technology. Thin-Walled Structures 36, 231–263.
Zienkiewicz, O.C., Taylor, R.L., 1991. The Finite Element Method, fourth ed. McGraw-Hill, London.